04,13,16

The structural electronic and thermodynamical properties of lithium-intercalated vanadium pentoxide

© E.M. Roginskii[1], A.V. Savin[1], E.A. Pankrushina[2]

[1] Ioffe Institute,
St. Petersburg, Russia
[2] Zavaritsky Institute of Geology and Geochemistry, Ural Branch of the Russian Academy of Sciences,
Yekaterinburg, Russia

E-mail: e.roginskii@mail.ioffe.ru

Received April 17, 2025
Revised May 30, 2025
Accepted May 31, 2025

The structural modifications of lithium-intercalated vanadium pentoxide are studied in detail. The dynamical, electronic, and thermodynamical properties of these materials are obtained using ab initio calculations. As a result, the structure and symmetry of the delta- and epsilon-Li-V_2O_5 polymorph are refined. The fingerprints in the high-frequency range of Raman spectrum which allows identifying the polymorph during the intercalation process is revealed. The calculation of thermodynamic properties within the quasi-harmonic approximation is performed. As a result, the main thermodynamic characteristics are obtained and the value of thermal conductivity for both the original vanadium pentoxide and the lithium-intercalated structure is estimated. It was found that the intercalation of the structure leads to a decrease in the phonon transport properties.

Keywords: cathodes, vanadium bronzes, thermodynamics.

DOI: 10.61011/PSS.2025.05.61490.86-25

1. Introduction

In the renewable energy sphere the most controversial is the issue of effective energy accumulation and its use when required. However, the problem of selecting the optimal material for a cathode still remains unsolved. In the industrial production the lamellar crystals Li_xMO_2 (here M — atom of transition metal) are used most widely as cathode material, for example, cathode from $LiFePO_4$ provides capacity of 165 mA h/g. The alternative may be the most thermodynamically stable vanadium oxide V_2O_5, which has a lamellar crystalline structure, determining its attractiveness as a cathode material.

Since they found it was possible to intercalate electrochemically lithium into matrix V_2O_5 (LiV_2O_5 bronzes), multiple studies were aimed at using intercalated structures as a cathode in batteries [1]. Due to the fact that the layers that vanadium pentoxide is made of are joined to each other with weak Van der Waals interaction, and vanadium atoms as such are in a group of transition metals with variable valency, the interaction process involves no substantial energy losses, which potentially provides high capacity and good electron conductivity [2].

It is known that when heated, LiV_2O_5 is exposed to some phase transitions [3]: δ-$LiV_2O_5 \longrightarrow \varepsilon$-$LiV_2O_5 \longrightarrow \gamma$-$LiV_2O_5$. It should be noted that chemical synthesis of vanadium bronzes usually results in formation of the most stable gamma-phase γ-LiV_2O_5, which differs substantially from phase δ-LiV_2O_5 in the structure of each layer. The latter is usually obtained by electrochemical intercalation of lithium in V_2O_5 [4], since such synthesis is accompanied with the minimum heat release. Structure δ-LiV_2O_5 was identified many times using X-ray diffraction analysis (see, e.g., [3–5]). Delta-phase of vanadium bronze δ-LiV_2O_5 maintains laminar structure (as in V_2O_5), but neighboring layers are moved towards each other in direction [010] by half of the lattice parameter ($b/2$). Therefore, the conclusion was made on preservation of the inversion center in the intercalated structure δ-LiV_2O_5, as well as in the volume V_2O_5, which assumes identical valency for all V atoms. The experiment determined space group of delta-phase — $Cmcm$, and the lattice cell is doubled in the direction perpendicular to layer [001]. However, the experiment [6] also considered the ordering of atoms in the delta phase structure without the inversion center, therefore, the question of unambiguous determination of the structural order remains open. Dynamic properties (obtained both from the experiment and calculations data) of the most stable phase γ-LiV_2O_5 are reported in many papers, while for delta-phase δ-LiV_2O_5, and for metastable ε-LiV_2O_5 there is no such data. This paper is dedicated to solving the issue of clarifying the structural parameters and symmetry of delta- and epsilon-phase of vanadium bronzes with the help of dynamic properties calculation within the density functional theory (DFT). The obtained structural parameters made it possible to further calculate the fundamental properties (electron structure, spectroscopic and thermodynamic properties) of these materials so critical for practical application.

2. Calculation parameters

The calculations based on the first principles were carried out within the framework of the density functional method using ABINIT program [7]. The calculations used functionals, the exchange-correlation part of which was described in the approximation of generalized gradients PBEsol [8]. The strongly correlated electron states (3d electrons of V atoms) were taken into account using Hubbard corrections to density functional [8], and the correction value was $U = 4$ eV. The calculations used optimized non-local (with two projectors of the non-local part), norm-preserving pseudopotentials [10]. The electrons in the orbitals $2s2p$ for the O atom and $3d4s4p$ for the V atom were considered as valence in the calculations. All-electron potential was used for lithium atoms. The cut-off energy in the calculation of the electronic structure was 35 Ha. The Monkhorst–Pack grids [11] were used for integration over the Brillouin zone in size $6 \times 6 \times 2$. The calculations involved complete relaxation of both atomic positions and lattice parameters. Relaxation was carried out until the forces acting on the atoms became less than $2 \cdot 10^{-5}$ Ha/Bohr with a self-consistent calculation of the total energy with an accuracy better than 10^{-8} Ha, and the deviation from zero pressure did not exceed 0.1 Kbar. Raman tensor and linear dielectric susceptibility were calculated within the perturbation theory [7].

The calculation of the Raman intensity of i-th vibrational mode in polarization $\gamma\beta$ was made using Placzek approximation [12] using the following expression:

$$I_{i\gamma\beta} = \frac{2\pi\hbar(\omega_L - \omega_i)^4}{c^4\omega_i}\,[n(\omega_i)+1]\,(\alpha^i_{\gamma\beta})^2, \qquad (1)$$

where $n(\omega_i)$ — Bose-Einstein occupation factor

$$n(\omega_i) = \frac{1}{e^{\hbar\omega_i/k_BT} - 1}, \qquad (2)$$

ω_L — frequency of excitation source, ω_i — frequency of i-th phonon, T — temperature, and α_{ij} — component of Raman tensor.

Since experimental spectra of intercalated phases are usually registered for polycrystalline specimens, it is necessary to use the averaged Raman tensor or rotational invariants of the second-rank tensor [12]:

$$\xi_i = \frac{1}{3}\left(\alpha^i_{xx} + \alpha^i_{yy} + \alpha^i_{zz}\right), \qquad (3)$$

$$\gamma_i^2 = \frac{1}{2}\left[(\alpha^i_{xx} - \alpha^i_{yy})^2 + (\alpha^i_{yy} - \alpha^i_{zz})^2 + (\alpha^i_{xx} - \alpha^i_{zz})^2\right] + \frac{3}{4}\left[(\alpha^i_{xy} + \alpha^i_{yx})^2 + (\alpha^i_{xz} + \alpha^i_{zx})^2 + (\alpha^i_{yz} + \alpha^i_{zy})^2\right], \qquad (4)$$

Then the intensity of the Raman spectrum lines for the parallel and crossed installation of polarizers is calculated using the following expressions:

$$I_i^{\perp} = \frac{2\pi\hbar(\omega_L - \omega_i)^4}{c^4\omega_i}\,[n(\omega_i)+1]\,\frac{\gamma_i^2}{15}, \qquad (5)$$

$$I_i^{\parallel} = \frac{2\pi\hbar(\omega_L - \omega_i)^4}{c^4\omega_i}\,[n(\omega_i)+1]\,\frac{45\xi_i^2 + 4\gamma_i^2}{45}. \qquad (6)$$

Accordingly, the full scattering intensity is $I_i^{tot} = I_i^{\parallel} + I_i^{\perp}$. In this paper the Raman light scattering spectra were calculated for polycrystalline specimens.

3. Structural properties

Crystalline vanadium pentoxide consists of O1-V-O2 chains, the form of which reminds a „ladder“, as shown previously in paper [13]. These „ladders“ are joined to each other by oxygen O3 atoms that serve as „bridges“, to form layers that create a volume crystal with space group (SG) *Pmmn* (#59) as shown in Figure 1. Vanadium atoms and O1 and O2 oxygen atoms occupy the Wyckoff positions $4f$, and „bridge“ O3 occupy a high-symmetry position $2a$. The structural parameters produced as a result of optimization compared to the experimental data are presented in Table 1.

According to the literature data, intercalation V_2O_5 with lithium atoms causes, first of all, introduction of the latter into the interlayer space, and second, to rebuilding of the structure related to the displacement of the layers towards each other along a short crystallographic axis by half of period, and delta-phase δ-LiV_2O_5 [6] finally occurs. X-ray diffraction analysis predicts two possible space groups for this structure, one is centrosymmetrical *Amam* (standard installation of the group — *Cmcm*) and non-centrosymmetrical $A2_1an$ ($Cmc2_1$ in a standard installation), where four formula units are contained. Due to ambiguity of the experimental data, the structure was chosen with the space centrosymmetric group *Cmcm* within this article for the calculations. According to [3], when temperature increases to $T_c = 433$ K, the rebuilding of structural nature takes place, which is accompanied by recovery of the mutual

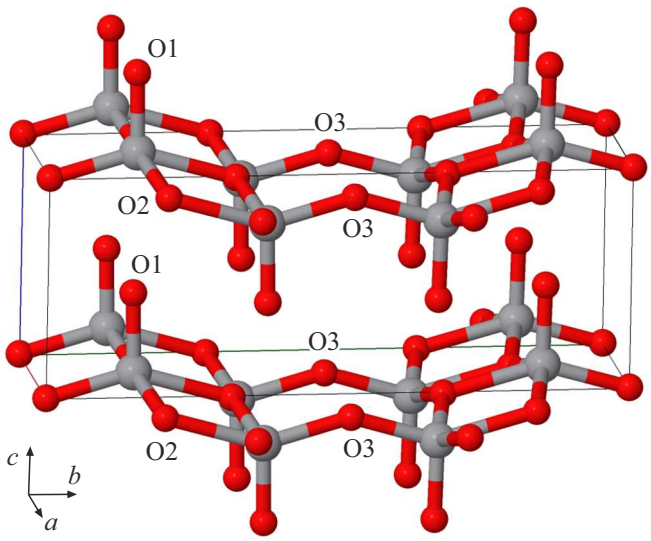

Figure 1. Lattice cell of crystalline V_2O_5. Grey balls — are vanadium atoms, small red balls — are oxygen atoms.

Table 1. Lattice parameters and coordinates of vanadium pentoxide α-V_2O_5 atoms coordinates

Parameter	Experiment [1]	LDA calculation [2]	GGA+U calculation
Lattice parameters			
a, Å	11.539	11.512	11.568
b, Å	3.572	3.564	3.568
c, Å	4.379	4.368	4.196
Positions of atoms, relative units			
V	(0.149, 0, 0.108)	(0.167, 0, 0.114)	(0.1491, 0, 0.1070)
O1	(0.15, 0, 0.471)	(0.168, 0, 0.486)	(0.1477, 0, 0.4868)
O2	(0.318, 0, 0.993)	(0.317, 0, 0.995)	(0.3138, 0, 0.9951)
O3	(0.0, 0, 0.006)	(0.0, 0, −0.004)	(0.0, 0, 0.0065)

Note. [1] Parameters from paper [14]. [2] Parameters from paper [15].

Table 2. Parameters of the lattice and coordinates of atoms of vanadium bronzes δ-LiV_2O_5 (PG *Cmcm*) and ε-LiV_2O_5 (PG *Pmmn*)

	δ-LiV_2O_5		ε-LiV_2O_5	
Parameter	Experiment[1]	Calculation of GGA+U	Experiment[2]	Calculation of GGA+U
Lattice parameters				
a, Å	3.6018	3.6008	11.3552	11.3005
b, Å	9.9055	9.8998	3.5732	3.5638
c, Å	11.2424	11.240	4.6548	4.5583
Positions of atoms, relative units				
V	(0, 0.2063, 0.5990)	(0, 0.2062, 0.6015)	(0.4002, 0.25, 0.8932)	(0.4011, 0.25, 0.8893)
O1	(0, 0.0464, 0.8731)	(0, 0.0460, 0.8739)	(0.1193, 0.25, 0.5510)	(0.1172, 0.25, 0.5371)
O2	(0.5 0.2626 0.9271)	(0.5, 0.2601, 0.9289)	(0.5733, 0.25, 0.9778)	(0.5725, 0.25, 0.9794)
O3	(0, 0.2856 0.75)	(0, 0.2843, 0.75)	(0.25, 0.25, 0.0293)	(0.25, 0.25, 0.0237)
Li	(0, 0.1092 0.25)	(0, 0.0961, 0.25)	(0.25, 0.75, 0.2845)	(0.25, 0.75, 0.2981)

Note. [1] Parameters from paper [6]. [2] Calculations from paper [3].

arrangement of layers, as in the initial non-intercalated V_2O_5 [3]. Such structure of vanadium bronze called epsilon-phase ε-LiV_2O_5. For ε-LiV_2O_5 the experiment also predict two close structures: centrosymmetric *Pmmn* and without the inversion center $P2_1mn$ ($Pmn2_1$ in the standard installation). This paper considered the structure of delta- and epsilon-phases containing the inversion center as the base. Structural parameters were optimized, and the results are available in Table 2 compared to experimental data. From the table you can see the good match of the calculations with the experimental data, however, note the underestimation of epsilon-phase lattice, which was caused by temperature expansion effect (experimental data ε-LiV_2O_5 were collected at 433 K). As it will be shown below, bronzes with such structural parameters are deemed to be unstable relative to the phonon spectrum, which indicates the need to clarity the structural parameters, mainly, determination of the availability of the inversion center.

4. Dynamic properties

Calculation of phonon spectrum δ-LiV_2O_5 in the center (Γ-point) and in the boundary point Z of Brillouin zone (BZ) demonstrated the availability of „unstable“ modes, the frequencies of which have imaginary value, which indicates the instability of a centrosymmetric structure *Cmcm*. Atomic displacements of imaginary modes are built in Figure 2.

You can see from Figure 2 that these „unstable“ modes are mainly characterized by displacement of O3 atoms, which bind V-O chains, and in case of a central zone phonon the O3 atoms are displaced in phase, and in case of an edge zone phonon the atoms are displaced in counterphase in the adjacent layers, which is rather expected since in the boundary point Z of BZ the phonon wavelength is equal to the lattice constant in direction perpendicular to the layer plane. In total four modes were found with imaginary frequency: two in the center and two at the boundary (in Z-point) of the Brillouin zone.

The presence of modes with imaginary frequencies in the phonon spectrum indicates the instability of these structural configurations, which do not comply with the energy minimum, the atomic displacement along the normal coordinates of „unstable“ modes causes no returning forces, but on the contrary results in energy reduction. However, such displacements lead to loss of some symmetry operations.

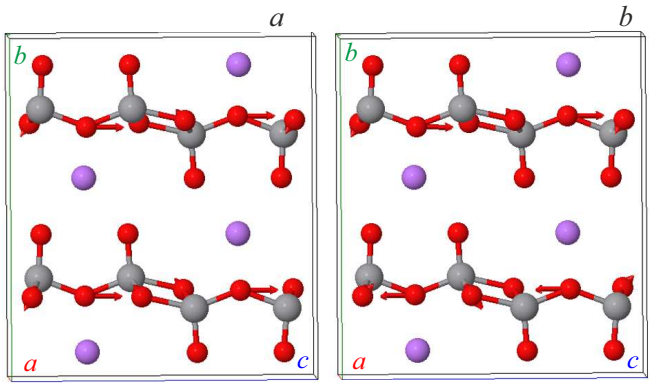

Figure 2. Atomic displacements of the vibrational mode in Γ-point of BZ with imaginary value of frequency i1080 cm^{-1} (*a*) and mode in *Z*-point of BZ with imaginary frequency i1062 cm^{-1} (*b*) of centrosymmetric phase δ-LiV_2O_5. Grey red and purple balls — atoms of vanadium, oxygen and lithium, respectively.

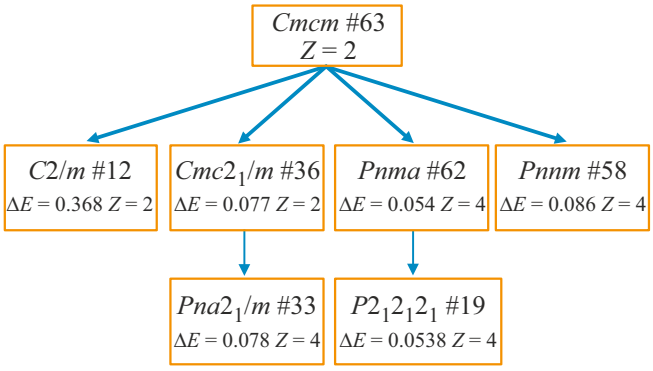

Figure 3. Group-subgroup diagram for parent phase δ-LiV_2O_5. ΔE — difference of the structure energy in respect to the parent phase, Z — number of formula units.

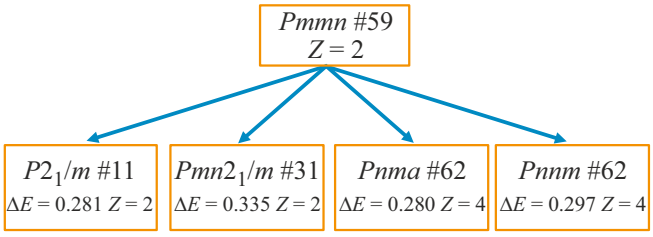

Figure 4. „Group-subgroup" diagram for parent phase δ-LiV_2O_5. ΔE — difference of the structure energy in respect to the parent phase, Z — number of formula units.

It is evident that when O3 atoms are displace (as shown in Figure 2), the inversion center operation is lost. Step-by-step distortion of the structure along the coordinates of modes with „imaginary" frequency with the increase of the displacement amplitude makes it possible to establish a more stable configuration from the energy point of view and to restore the symmetry of the obtained structure.

The paper conducted the above procedure to search for stable configurations δ-LiV_2O_5 by distortion of the parent structure *Cmcm* along the vectors of atomic displacements of „imaginary" modes. The symmetry of each distorted structure was established, and structural parameters were optimized with subsequent calculation of the phonon spectrum and full energy of the produced polymorph. The diagram „group-subgroup" (link of the parent phase with derivative polymorphs) is given in Figure 3. It should be noted that in the spectra of structures with PG $Cmc2_1$ and *Pnnm* the modes were found again with imaginary frequencies, therefore, the distortion operation was again performed along the imaginary modes. As a result, the subgroups $Pna2_1$ and $P2_12_12_1$ were obtained.

From the diagram of Figure 3 you can see that the structures with symmetry *Pnnm*, $Cmc2_1$ and $Pna2_1$ are characterized by minimum energy. Besides, differences of the structure with PG $Pna2_1$ from the structure with PG $Cmc2_1$ coincide with the accuracy of up to 0.01 Å, and the difference in the energy is less than 0.001 eV, therefore, from the point of view of the structural order these structures may be deemed identical. Since the experimental paper [6] mentions $Cmc2_1$ group, all further calculations were made for this group. Since the experiment was performed at room temperature, and the calculations of dynamic properties were implemented in harmonic approximation, you may assume that as the temperature decreases, phase $Pna2_1$ becomes more beneficial by energy, which contributes to the low-temperature structural phase transition (PT).

The similar procedure was performed for bronze ε-LiV_2O_5. The result of such analysis is presented in the „group-subgroup" diagram in Figure 4.

From the diagram it follows that the most beneficial is the structure with symmetry $Pmn2_1$, this is exactly the group seen as one of the possible ones in the experiment [3]. Therefore, according to the calculations, both delta- and epsilon-phase LiV_2O_5 demonstrates the absence of the inversion center, this circumstance determines the rules of selection in the Raman scattering spectroscopy.

5. Electronic structure, dielectric properties and spectroscopy

Electronic structure of V_2O_5, intercalated with lithium, was studied previously in paper [16], but for a gamma phase, which differs substantially in the structure from the delta and epsilon phases considered in this paper. In bronze γ-LiV_2O_5 the layers undergo severe deformation, therefore, the electronic structure may differ up to manifestation of metallic properties. To clarify the situation, calculations of the electronic zonal structure of delta and epsilon phase were conducted, and the results of the calculation for ε-LiV_2O_5 are presented in Figure 5. As you can see in the figure, the direct optical transition in Γ-point of BZ is not fundamental, the transition from the valence band to the conduction band with the least energy is carried out in

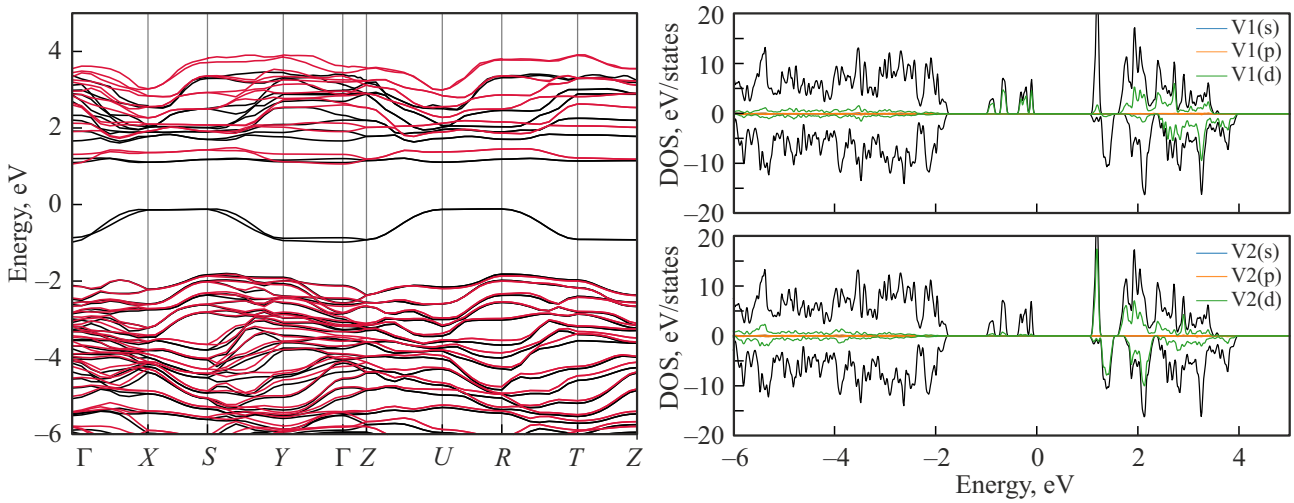

Figure 5. Electronic zone structure ε-LiV_2O_5 (on the left) and density of electron states (on the right). The energy scale is built relative to the Fermi energy. Black and red branches in the zone structure correspond to the states with the upward and downward spin, respectively. Black curves in the curve of the density of states correspond to the total contribution, and blue, red and green curves — projection of stages onto s-, p- and d-states of vanadium atoms. The states with the downward spin for more visibility are built with a negative sign.

BZ boundary points (X, S, U, R). Besides, the fundamental phase transition is observed in the X point with the band gap value $E_g = 1.04$ eV, this point has a coordinate (0.5 0 0) in the reciprocal space, which means that the fundamental optical properties are determined by the structure of a separate layer.

The specific feature of vanadium bronzes is a narrow valence band, which consists of only several branches, and these branches correspond to the states with the separated spin. In the zone structure built in Figure 5, these branches are in the area of energies near Fermi level (indicated with black color). To explain the nature of these branches, the total density of electron states (DOS) was calculated with subsequent projection onto atomic orbitals (projection densities). The result is given in the fight part of Figure 5. As you can see from the figure, the discussed narrow valence band is formed by electrons, localized in d-orbitals of transition metal V. Besides, since the thermodynamically stable phase $Pmn2_1$ contains two symmetrically nonequivalent atoms V, each occupying Wyckoff positions $2a$, the projections of density of electron states were built for two symmetrically nonequivalent atoms V. The analysis of the curves has shown that namely d-electrons of the first type of atoms V1 provide the decisive contribution to the highest energy valence band, while the d-electrons of vanadium atoms of the second type V2 contribute to the lowest energy conduction band. Therefore, it is evident that structure ε-LiV_2O_5 contains two types of symmetrically nonequivalent vanadium atoms with different valence state $V1^{4+}$ and $V2^{5+}$. Similar situation is observed for noncentrosymmetric delta phase $Cmc2_1$ δ-LiV_2O_5, the difference is only in the width of the band gap $E_g = 1.09$ eV. Such similarity of the electronic structure of two polymorphs is explained by the fact that as noted above the electronic properties depend on the structure of an individual layer, and the layers in the considered epsilon and delta phases are identical, the difference is in their mutual arrangement.

Due to the lamellar nature of the vanadium bronze structure in these crystals, the calculation of dielectric properties demonstrated strong anisotropy of a dielectric tensor, the value of diagonal components in which within the disturbance theory for δ-LiV_2O_5 was $\varepsilon_{xx} = 3.39$, $\varepsilon_{yy} = 4.77$, $\varepsilon_{zz} = 6.05$. The produced values for ε-LiV_2O_5 are equal to $\varepsilon_{xx} = 4.88$, $\varepsilon_{yy} = 3.89$, $\varepsilon_{zz} = 6.09$. Taking into account the fact that the crystallographic axes of delta and epsilon phase in the plane of the layer in process of transition from one phase to the other are transformed by the operation of rotation by 90 degrees, the dielectric properties of phases are hardly discernible. Therefore, you can conclude that dielectric abnormalities are absent in the vanadium bronzes in a phase transition.

The point group of thermodynamically stable phases of vanadium bronzes $mm2$ „permits“ the presence of nonzero square nonlinear susceptibility $\chi^{(2)}$, however, the study of nonlinear optical properties is a complicated task, which deserves a separate precision study, therefore, this paper did not estimate the values of nonlinear susceptibility tensor. Nevertheless, another just as important property of the material is the response of crystal linear susceptibility to atomic displacements specific for a certain vibrational mode. It should be noted that this is also a nonlinear process well known as vibrational spectroscopy.

Raman scattering spectroscopy (RSS) — is a precision method making it possible to detect the local changes in the structural parameters as a result of any exposure of the substance, for example, as a result of a structural phase transition. RSS was calculated for epsilon and delta phases LiV_2O_5, and the result is built in Figure 6.

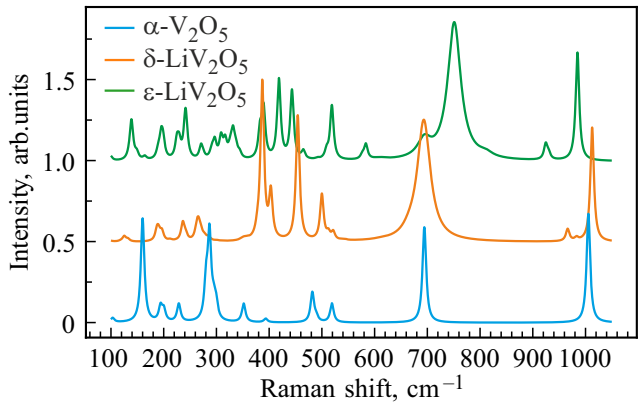

Figure 6. Raman scattering spectra of epsilon and delta polymorph LiV_2O_5, calculated for thermodynamically stable $Cmc2_1$ and $Pmn2_1$ phases, compared to the calculated spectrum of the source powder α-V_2O_5.

According to the theoretical group analysis, the decomposition of phonons in the BZ center with irreducible representations (IR) of delta- ($Cmc2_1$) and epsilon-phases (PG $Pmn2_1$) is as follows:

$$\Gamma = 15A_1 \oplus 8A_2 \oplus 7B_1 \oplus 15B_2, \qquad (7)$$

where all modes, except for those converted according to IR A_2, are optically active.

Despite the identity of decomposition, the spectra have substantial differences in the high-frequency area, where a doublet is observed, which consists of a strong line and a weak satellite in a low-frequency wing. Besides, the difference in the position of these intense lines of two phases is approximately $25\,cm^{-1}$. It should be noted that the displacement of a high-frequency line of delta-phase in respect to the position of the line of source V_2O_5 is observed towards the frequency increase, and for epsilon phase the displacement takes place towards the low-frequency area. Figure 7 built vectors of atomic displacements of vibrational modes, corresponding to the most intense high-frequency lines in the RS spectrum. As you can see in Figure 7, these modes are valence oscillations V1-O1 (V2-O1), where O1 oxygen atomic displacements happen along the link. It should be noted that the length of the link V1-O1 is the shortest in bronzes, therefore these valence oscillations are the highest frequency ones.

Remember that epsilon- and delta-phases differ by mutual location of the layers along the short crystallographic axis. Displacement of one layer relative to the other layer by half of the period in ε-LiV_2O_5 results in the fact that the density formed by atoms O1-Li-O1 (as shown in Figure 7), is no longer perpendicular to the plane of the layer, which causes weakening in the interaction of O1 atoms and the closest Li. Weaker interaction results in softer frequency, which explains the difference in frequencies of valence oscillations in epsilon- and delta-phases. Previously, in paper [17], the RS spectrum was recorded experimentally for the partially intercalated structure ε-$Li_{0.52}V_2O_5$ and δ-LiV_2O_5. Comparison of the experimental spectra of bronzes with the spectrum of volumetric α-V_2O_5 in the high-frequency area (Figure 4, 8 of article [17]) demonstrates the above trend that once again confirms the validity of the results obtained in this paper.

Table 3. Values of frequencies of centerband phonons that contribute substantially to the RSS, calculated within the density functional theory compared to data from the experiment [17]

№	δ-LiV_2O_5			ε-LiV_2O_5		
	IR	DFT	Experiment	IR	DFT	Experiment
1	A_1	124	145	B_1	138	154
2	B_2	196		A_1	189	
3	A_2	236		B_2	194	
4	A_1	265		A_1	230	218
5	A_2	269	271	A_2	241	
6	A_1	386	355	B_1	270	284
7	A_1	402	420	A_2	296	
8	A_1	452	435	B_2	308	300
9	A_1	499		A_1	316	
10	A_1	519	533	A_2	331	
11	B_1	660	630	A_1	389	
12	A_1	691	690	A_1	418	420
13	A_1	965		A_1	443	486
14	B_2	982	973	A_1	519	535
15	A_1	1013	1008	B_1	583	
16				B_2	609	
17				B_1	692	
18				A_2	695	703
19				A_1	750	
20				A_1	924	
21				A_1	984	983

Table 3 includes the frequencies of vibrational modes that correspond to the intense peaks in RS spectra obtained in this calculation, compared to the experiment from paper [17]. In general, it is possible to relate all peaks observed in the experiment to the vibrational modes obtained in the calculations. It is expected that the most intense lines in the spectra are converted using a fully symmetric irreducible representation A_1. Nevertheless, it is possible to observe the lines that are related to oscillations with symmetry A_2 and B_1 in the experimental spectra. It should be noted that it is not possible to experimentally resolve all lines from the calculated spectrum, which may be explained by a relatively large half-width of the lines and low signal/noise ratio. Besides, according to the data from paper [17], the specimens are exposed to degradation when high capacities of the light source are used, and the small value of the band gap of vanadium bronzes may cause resonance effects due to photon-electron interaction as discussed in paper [16], these circumstances create certain difficulties in the experimental spectroscopy. Nevertheless, due to good reproduction of the experimental spectrum, you

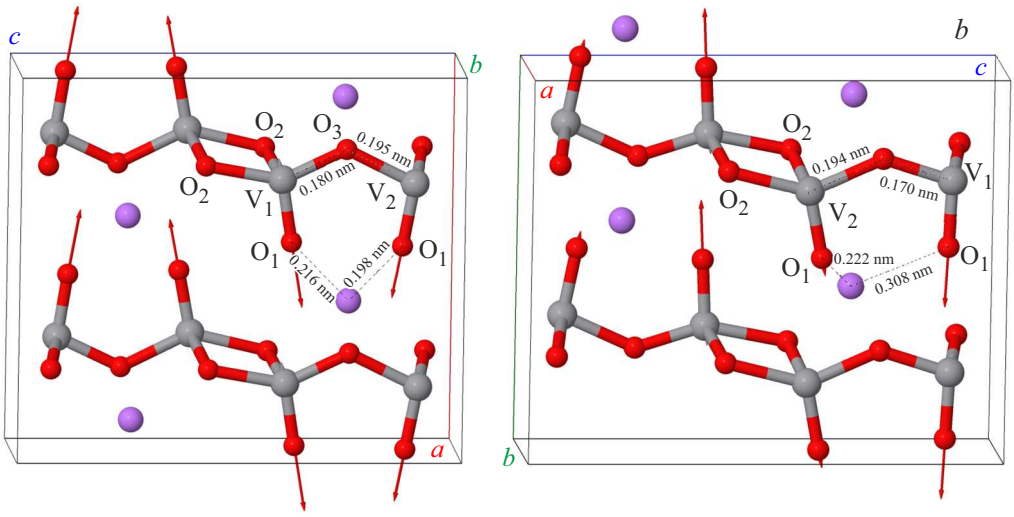

Figure 7. Atomic displacements corresponding to oscillations in δ-LiV_2O_5 with frequency 1012.5 cm^{-1} (IR A_1) (on the left) and displacements for the mode with frequency of 984.7 cm^{-1} in ε-LiV_2O_5 (IR A_1) (on the right).

may conclude on the low concentration of defects in the experimental crystalline phases or their complete absence.

Therefore, using Raman scattering spectroscopy you can determine the spatial structure of vanadium bronzes in process of intercalation in real time mode.

The spectrum includes a line in the area of 700 cm^{-1}, which could also serve a reference point in analysis of the composition, however, as it is shown in paper [16], this line is of resonant nature in the experimental spectrum of gamma phase γ-LiV_2O_5 and depends on the source of excitation, therefore, this line is not suitable for determination of the vanadium bronze polymorph structure.

6. Thermodynamic properties

Since when the material is used as a cathode, it is important to properly determine the operating conditions, the calculations of thermodynamic properties of vanadium bronzes were made within quasi-harmonic approximation. In this approximation the temperature effects are calculated by accounting for the free energy of phonons. Helmholtz free energy $F(T,V) = E_{DFT} + F_{ph}(T,V)$ includes two contributions, full energy of the system at the specified volume of the lattice cell V and energy of phonons $F_{ph}(T,V)$, which depends on the volume of the lattice cell and temperature:

$$E = \sum_{\mathbf{q}\nu} \hbar\omega(\mathbf{q}\nu)\left[\frac{1}{2} + \frac{1}{\exp(\hbar\omega(\mathbf{q}\nu)/k_B T) - 1}\right], \qquad (8)$$

where Bose-Einstein occupation factor is:

$$n = \frac{1}{\exp(\hbar\omega(\mathbf{q}\nu)/k_B T) - 1}. \qquad (9)$$

It should be noted that the definition of the dependence of phonon free energy on the volume and wave vector requires calculation of the phononic dispersion for the structures with the various value of the lattice cell volume, which is a resource-intensive task. The obtained dependence $F(T,V)$ is approximated analytically for each temperature in the range from 0 to 1000 K, using which, the equilibrium volume of the cell is determined, corresponding to the free Helmholtz energy minimum. As a result, the dependence of the lattice cell volume on temperature was obtained, which made it possible to obtain the temperature dependence of heat capacity at constant pressure C_p. Figure 8 built a temperature dependence of the calculated heat capacity compared to the experiment. The figure shows good reproduction of literature data, which means satisfactory de-

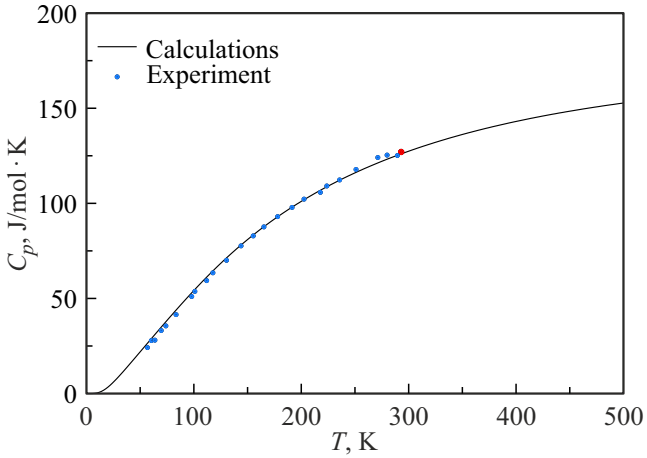

Figure 8. Temperature dependence of heat capacity C_p of vanadium pentoxide calculated in quasi-harmonic approximation (solid line) compared to the experiment. Blue dots — experiment from paper [18], red dot — from paper [19].

scription of thermodynamic properties of vanadium bronzes using the selected theoretical approach.

Another important parameter determining the processes of ion transfer due to phonons is Gruneisen parameter:

$$\gamma(\mathbf{q}\nu) = -\frac{V}{\omega(\mathbf{q}\nu)}\frac{\partial\omega(\mathbf{q}\nu)}{\partial V}. \quad (10)$$

This parameter is calculated using the finite difference technique from the dispersion of phononic branches for three structures with different volumes of the lattice cell. Then the parameter is averaged by all phononic states in the entire Brillouin zone. The obtained value at room temperature for V_2O_5 was $\gamma = 0.59$, which is approximately three times less than the Gruneisen parameter in gallium oxide [20]. Since the medium and high frequency area of the phononic spectrum in V_2O_5 is defined by the layer properties, a relatively small value γ indicates weak change of structural parameters of an individual layer. The structure deformation is mostly incident upon the interplanar spacing, which determines the low frequency area of the oscillation spectrum.

In order to assess the thermal conductivity value of vanadium bronzes, you may use the empirical Slack–Morelli formula [21], which demonstrated successful use for a wide spectrum of materials:

$$\kappa_L = A\frac{MT_D^3\delta}{\gamma^2 N^{2/3}T}, \quad (11)$$

where N — number of atoms in a lattice cell, δ^3 — volume of a cell related to a number of atoms, M — average molar mass of a formula unit, and the empirical parameter A is specified by the expression:

$$A = \frac{2.43\cdot 10^{-8}}{1 - 0.514/\gamma + 0.228/\gamma^2}, \quad (12)$$

T_D — Debye temperature, which is determined based on the temperature dependence of heat capacity as the saturation temperature.

The thermal conductivity value V_2O_5 obtained in this manner at room temperature is equal to $\kappa = 2.4$ W/mK, which agrees well with the experimental data from paper [22], where the thermal conductivity value at temperature $T = 500$ K was $\kappa = 1.8$ W/mK.

A similar approach was applied to vanadium bronzes, as a result of which the Gruneisen parameter value $\gamma = 0.3$ was found, and the thermal conductivity value was $\kappa = 1.7$ W/mK, which is approximately 30 % below the value obtained for pure V_2O_5. Accordingly, you can assume that as a result of structure intercalation with alkali metals the thermal conductivity value decreases, which indirectly specifies the increase of anharmonicity extent in vanadium bronzes.

7. Conclusion

The results of a comprehensive study of the structural, electronic, and dielectric properties of vanadium bronzes are presented in this paper. Structural, electronic, and thermodynamic properties of vanadium bronzes Li-V_2O_5 are theoretically studied using non-empirical quantum-mechanical calculations. The study of the structural properties made it possible to clear unambiguity in the experimental definition of delta- and epsilon-phase symmetry. Vibrational modes were found in the spectrum of centrosymmetric structures that indicate the instability of such spatial ordering. It was established that structures with spatial groups $Cmc2_1$ and $Pmn2_1$ for delta and epsilon phases, respectively, are thermodynamically stable. Absence of the inversion center in the obtained structures and analysis of projections of density of electron states indicates presence of two types of vanadium atoms in the structure with the valence of 4+ and 5+, as in the case of the well studied gamma phase. Modeling of the Raman scattering spectra found a specific feature in the high-frequency area of the spectrum, which makes it possible to identify a polymorph in process of intercalation. Calculation of the thermodynamic properties within quasi-harmonic approximation made it possible to determine the main thermodynamic characteristics and to assess the thermal conductivity value both for the source vanadium pentoxide and for the structure intercalated with lithium.

Acknowledgments

The study was performed using computing resources of the supercomputer in Ioffee Physical-Technical Institute.

Funding

E.A. Pankrushina would like to express gratitude to the Russian Science Foundation for financial support (grant No. 24-73-00009).

Conflict of interest

The authors declare that they have no conflict of interest.

References

[1] M.S. Whittingham. J. Electrochem. Soc. **123**, 315 (1976).
[2] E. Esparcia, J. Joo, J. Lee. CrystEngComm **23**, 5267 (2021).
[3] C. Satto, P. Sciau, E. Dooryhee, J. Galy, P. Millet. J. Solid State Chem. **146**, 103 (1999).
[4] J. Cocciantelli, M. Menetrier, C. Delmas, J. Doumerc, M. Pouchard, P. Hagenmuller. Solid State Ion. **50**, 99 (1992).
[5] S. Caes, J.C. Arrebola, N. Krins, P. Eloy, E.M. Gaigneaux, C. Henrist, R. Cloots, B. Vertruyen. J. Mater. Chem. A **2**, 5809 (2014).
[6] R. Cava, A. Santoro, D. Murphy, S. Zahurak, R. Fleming, P. Marsh, R. Roth. J. Solid State Chem. **65**, 63 (1986).

[7] X. Gonze, B. Amadon, P.-M. Anglade, J.-M. Beuken, F. Bottin, P. Boulanger, F. Bruneval, D. Caliste, R. Caracas, M. C.ot.e, T. Deutsch, L. Genovese, P. Ghosez, M. Giantomassi, S. Goedecker, D. Hamann, P. Hermet, F. Jollet, G. Jomard, S. Leroux, M. Mancini, S. Mazevet, M. Oliveira, G. Onida, Y. Pouillon, T. Rangel, G.-M. Rignanese, D. Sangalli, R. Shaltaf, M. Torrent, M. Verstraete, G. Zerah, J. Zwanziger. Comput. Phys. Commun. **180**, 2582 (2009).
[8] J.P. Perdew, A. Ruzsinszky, G.I. Csonka, O.A. Vydrov, G.E. Scuseria, L.A. Constantin, X. Zhou, K. Burke. Phys. Rev. Lett. **100**, 136406 (2008).
[9] A.I. Liechtenstein, V.I. Anisimov, J. Zaanen. Phys. Rev. B **52**, R5467 (1995).
[10] D.R. Hamann. Phys. Rev. B **88**, 085117 (2013).
[11] H.J. Monkhorst, J.D. Pack. Phys. Rev. B: Condens. Matter Mater. Phys. **13**, 5188 (1976).
[12] M. Born, R. Huang. Dynamical Theory of Crystal lattices, Oxford University Press (1954).
[13] M.B. Smirnov, E.M. Roginskii, V.Y. Kazimirov, K.S. Smirnov, R. Baddour-Hadjean, J.P. Pereira-Ramos, V.S. Zhandun. J. Phys. Chem. C **119**, 20801 (2015).
[14] X. Shan, S. Kim, A.M.M. Abeykoon, G. Kwon, D. Olds, X. Teng. ACS Appl. Mater. Interfaces **12**, 54627 (2020).
[15] B. Zhou, D. He. J. Raman Spectrosc. **39**, 1475 (2008).
[16] E.M. Roginskii, M.B. Smirnov, K.S. Smirnov, R. Baddour-Hadjean, J.-P. Pereira-Ramos, A.N. Smirnov, V.Y. Davydov. J. Phys. Chem. C **125**, 5848 (2021).
[17] R. Baddour-Hadjean, E. Raekelboom, J.P. Pereira-Ramos. Chem. Mater. **18**, 3548 (2006).
[18] C.T. Anderson. J. Am. Chem. Soc. **58**, 564 (1936).
[19] W.M. Haynes. CRC Handbook of chemistry and physics, CRC Press, 95 edition (2014).
[20] Q. Liu, Z. Chen, X. Zhou. ACS Omega **7**, 11643 (2022).
[21] D.T. Morelli, G.A. Slack. High lattice thermal conductivity solids in high thermal conductivity materials, Springer-Verlag (2006).
[22] V.I. Fyodorov, I.Ya. Davydov. Teplofizicheskiye svoistva veschestv **16**, 765 (1978). (in Russian).

Translated by M.Verenikina